Empirical and Numerical Investigation of Turbulent Flows in a Novel Design Burner for Ammonia/Hydrogen Combustion

M. Kovaleva[*, 1], S. Mashruk[1], A. Valera-Medina[1],

[1]College of Physical Sciences and Engineering, Cardiff University, Cardiff, UK

Abstract

Ammonia-hydrogen fuel blends are an attractive option for the decarbonization of the energy sector with improved combustion characteristics over pure ammonia fuels. However, further research into methods of reducing NO_x and NH_3 emissions is necessary for combustors operating with these fuel blends. This paper details a novel burner design for partially premixed ammonia-hydrogen fuel injection incorporating considerations for waste heat, unburnt ammonia and improved combustion residence times. Laser Doppler anemometry (LDA) and computational fluid dynamics using a 3D RANS realizable k-epsilon (k-ε) model were employed to characterise the three-dimensional isothermal flow field of the design. The results show a promising flow profile with an anchored flame, a central recirculation zone and increased residence times.

Introduction

Of the many hydrogen carriers available today, ammonia is considered to be one of the cheapest storage and transportation vectors with established infrastructure across many industries [1]. In the past, ammonia's popularity as a green hydrogen carrier fuel has been hindered by its low reactivity. However, recent studies have shown that ammonia's combustion characteristics can be improved by doping with a more reactive fuel such as hydrogen and methane, leading to a surge of renewed interest in this fuel.

In an effort to achieve low NO_x and NH_3 emissions with ammonia-hydrogen fuel blends, researchers have considered various adaptations to combustor designs. Some of these low NOx technologies have been in use since the 1970s and 1980s [2]. However, their implementation still requires further understanding of ammonia-hydrogen power flame dynamics and chemistry [3].

This study follows previous investigations conducted at Cardiff University in optimising ammonia-hydrogen combustion, focused on 70-30 (vol%) ammonia-hydrogen fuel mixtures as a compromise between flame stability and heat release rate. Valera-Medina et al. [4] compared the Brayton cycle efficiency of this fuel mixture with a more traditional methane-based system using Dry Low NOx (DLN) technologies. The results showed a strong need to explore more advanced injection configurations in order for ammonia-hydrogen power plants to be competitive with existing hydrocarbon solutions. Another study of this fuel mixture by Pugh et al. [5] recommends a partially premixed injection method, a primary zone equivalence ratio of 1.2 and various hydrogen addition strategies.

Steam injection has also been explored as a method of increasing efficiencies in these systems. Guteša Božo et. al [6] studied the injection of ammonia-hydrogen for up to 0.72 steam/fuel mass ratio, reaching overall plant efficiencies of ~34%. Furthermore, as steam was increased, there was an increase in the portion of ammonia that was burnt in the secondary zone, as well as an increase in the portion of OH radicals and NH_2 radical production and reduced temperatures (and hence thermal NO_x production routes). All of the above contributed to an overall reduction in NO_x. Considering these results, further studies have also demonstrated the viability of below 100 ppm NOx emissions for a humidified RQL combustion configuration at an industrial scale ~10MW, through a reversed Brayton gas turbine plant facility [7, 8].

Kurata et al. [9, 10], gave the first modern demonstration of ammonia and ammonia-kerosene combustion in a real micro gas turbine (MGT) using selective catalytic reduction (SCR) for NO_x reduction. Groups in Japan have since gone on to study methods of NOx reduction in pure ammonia systems. Somarathne et al. [11] studied the effect of pressure on ammonia fuelled staged combustors to also find an optimal injection equivalence ratio of 1.15 – 1.2, while Okafor et. al [12] studied the effect of various combustor parameters on pure ammonia combustion. It was shown that an inclined injection angle (specifically 45 °) improved combustion efficiencies and gave a good compromise between emissions and liner temperatures. This study also recommends the rich-lean configuration, with an optimum primary zone equivalence ratio of 1.10 and overall equivalence ratio of 0.40 to 0.67.

Rocha et al. [13] also used numerical modelling to compare pure ammonia combustion with DLE, RQL and moderate low oxygen dilution (MILD) technologies, showing the best performance for the MILD and RQL configurations. One final concept of interest is the use of a porous medium burner in stabilising ammonia-hydrogen flames, with the potential to broaden the flame stability region for larger burner diameters and increase power densities [14]. While extending flammability limits of lower heat fuels is an inherent advantage of this type of burner, it is less common for high power gas turbine applications, and so has not been explored further in the present study.

Swirl burners are commonly used for gas turbine applications, but these are relatively new for ammonia-

* Corresponding author: kovalevam@cardiff.ac.uk

hydrogen combustion, with limited studies. Therefore, the present work explores the performance of NIK15, a novel NH_3/H_2 burner designed for RQL injection to guide the future development of gas turbine combustors that meet stringent requirements of the EU Industrial Emissions Directive [16].

Method

The hydrodynamic testing of swirling flows was conducted experimentally at Cardiff University Thermofluids Laboratory. The burner design was based on a modified swirl burner (with a swirl number of ~0.8) and separate inlets for premixed ammonia-hydrogen-air to achieve a stratified partially-premixed injection configuration. 1D Laser Doppler anemometry (LDA) was conducted for an inlet air velocity of 300L/min, equivalent to 16.8kW at an equivalence ratio of 1.2 with 70-30 (vol%) ammonia-hydrogen by fuel volume fraction.

Velocity profiles were measured utilising a dedicated Windows Software Package - BSA Flow Software, for data acquisition. A measurement grid for multiple axial (x – y) and cross-sectional (x – z) planes was used for analysing radial (i) , tangential (j) and axial (k) velocity vectors. A grid of 40mm on the x-axis (with density of 1mm) and 18 to 40mm on the y-axis and z-axis (with density of 3mm) was taken for the measurements. In each case, the seeding particles, (i.e., aluminium oxide), were maintained at 10,000 counts, which was far above the required minimum accuracy level of 2,000.

Star-CCM+ v20.3.1 was employed for computational fluid dynamics modelling of the burner. A variety of two equation models were tested. Of these, the realizable two-layer k-epsilon (k-ε) two equation model showed the best agreement to the experimental data and was selected for the following study.

Table 1 – Boundary conditions

Parameter	Value
Swirler walls	Adiabatic
Burner section	Symmetry (120°)
Swirler walls	Adiabatic
Inlet velocity	1.30 m/s
Inlet temperature	300K
Method	Segregated flow, isothermal
Walls	No slip
Swirl	0.8
Blend	70-30 (vol%) ammonia-hydrogen

To minimize computational requirements, 1/3 of the burner was used with periodic boundary conditions. To match the LDA configuration, the burner was unconfined with an extended computational domain with symmetry walls, Figure 1. A mesh size of 2.9 million cells was selected with a higher mesh density for the flame zone and near-flame areas containing high velocity gradients and kinetic energy residual values. This higher density mesh coincided with the area for which LDA measurements were taken and the most extreme velocity gradients were located.

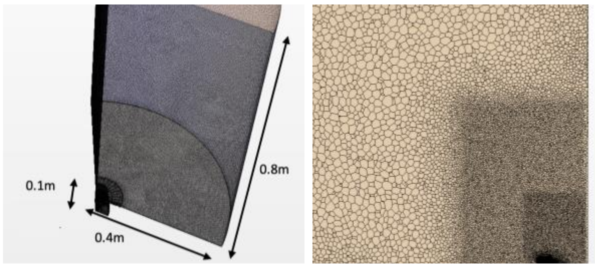

Figure 1 – generated mesh with computational domain and burner dimensions.

Table 2 – Cell count for mesh sensitivity

Mesh type	Number of cells
course	1,082,072
medium	2,907,516
fine	6,240,540

The course mesh was not able to capture the burner geometry in sufficient detail. However, an increase in mesh density between the medium and fine mesh did not have a significant impact on the result (as shown by Figure 2), therefore the medium mesh was sufficient for the following analysis.

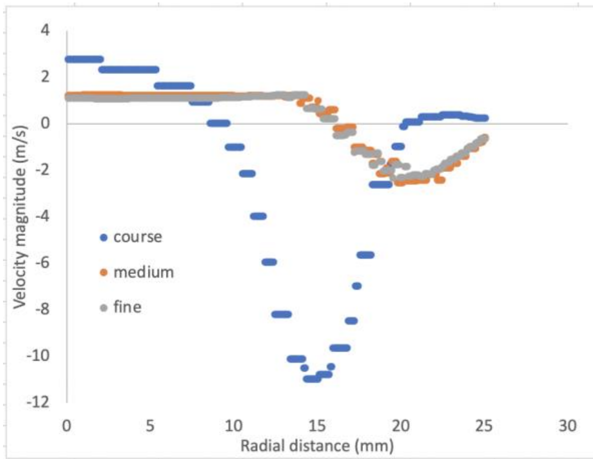

Figure 2 – Mesh sensitivity analysis

Results and Discussion

Figure 3 shows the velocity magnitude on the axial plane (x – y) with respect the axial (k) direction. The experimental data shows a central area of negative velocity implying a central recirculation zone and a lower corner on the other side of the jet to suggest the presence of an outer recirculation zone. The jet angle is at approximately 45° and flattens further at the tip for increased mixing and residence times.

A comparison of experimental and numerical data shows the same trends, velocity profiles across and coherent structures across the axial plane. Along the base (y = 0 line), velocity magnitude peaked at the same location for around 8-10 m/s magnitude. One key difference is that the jet height is lower in the numerical simulation, giving a lower peak velocity at the base.

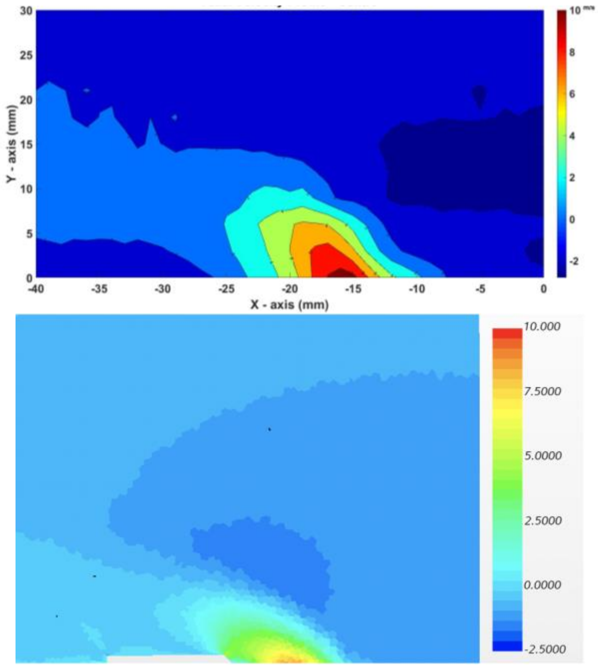

Figure 3 – Experimental (top) and numerical (bottom) profile of axial velocity vector on the axial plane

Figure 4 shows the axial planes taken at various depths in the z direction away from burner centre. There is limited distinction in the experimental results for these planes.

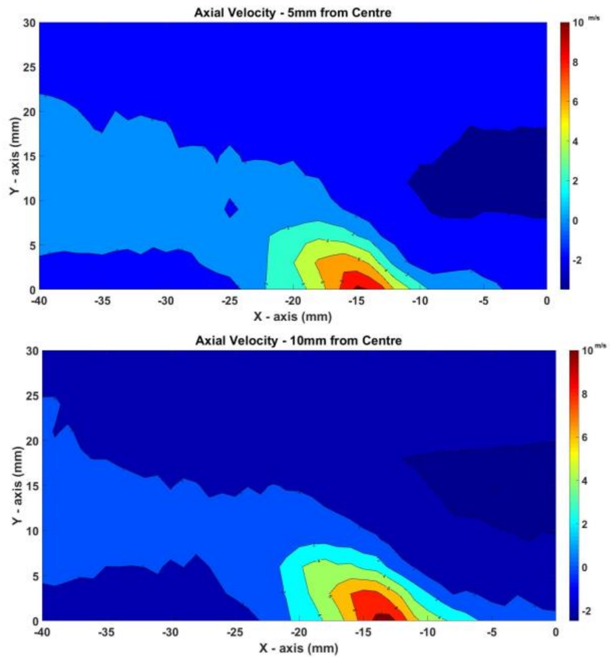

Figure 4 – experimental velocity profiles for axial planes cut at 5mm depth (top), 10mm depth (bottom)

The numerical model shows even less change across different planes, with an almost identical profile and magnitudes even up to 30mm from the centre (Figure 5). In all cases, the jet close to the burner is almost entirely unaffected with the most difference at the jet tip. This suggests a stable and even flame around the full circumference of the burner.

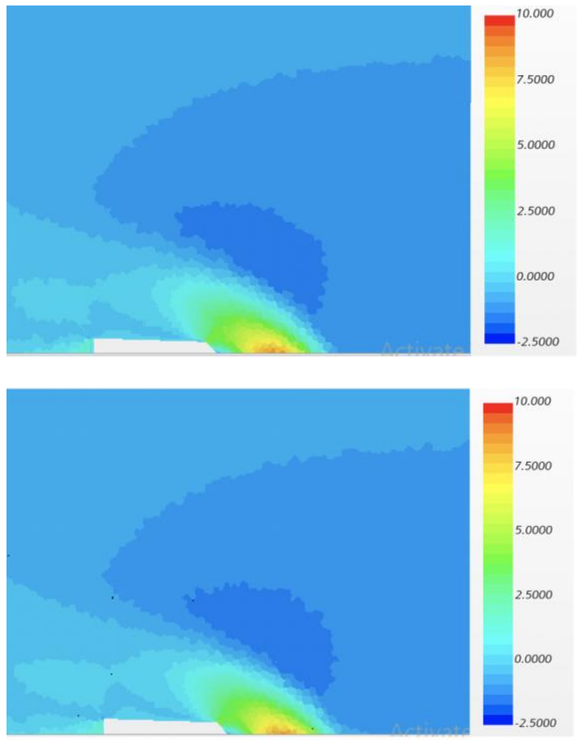

Figure 5 Numerical velocity profiles for axial planes cut at 10mm (top), 30mm (bottom) from the central plane

The radial/tangential plane (x – y) through the burner cross-section was also studied. This plane height corresponds to y = 0mm on axial plane images. This data shows intersecting flows from opposing directions (Figures 6). The magnitude of the tangential velocities are as high as axial velocities at this height with the locations matching, also suggesting a flattening of the jet.

The profiles and magnitude of these flows match for both experimental and numerical results. Due to the definition of the tangential velocity vector, this pattern is likely to follow a cyclic pattern with the positive and negative velocity peaks carrying the same shape. Due to the use of a 1/3 section mesh of the original profile, the full extent of the negative velocity zone cannot be viewed with the CFD model. This difficulty in alignment is likely to be the largest source of error in the radial and tangential velocity vectors.

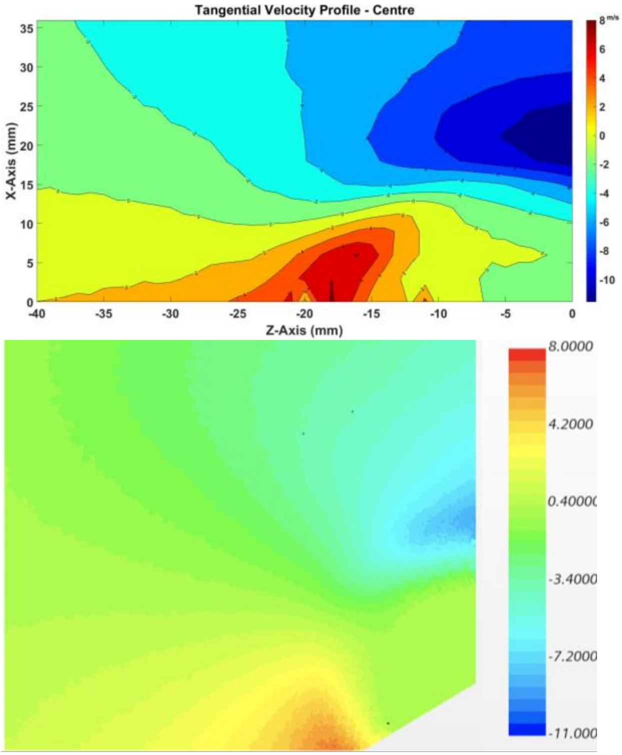

Figure 6 – Experimental (top) and numerical (bottom) profile of tangential velocity vector on the cross-sectional plane.

Finally, the radial and tangential velocity vectors on the axial plane were explored. Experimental results showed peak radial velocity occurring at a height of 6mm above the burner edge and at a larger burner radius in comparison to the axial velocity vector peak (Figure 7).

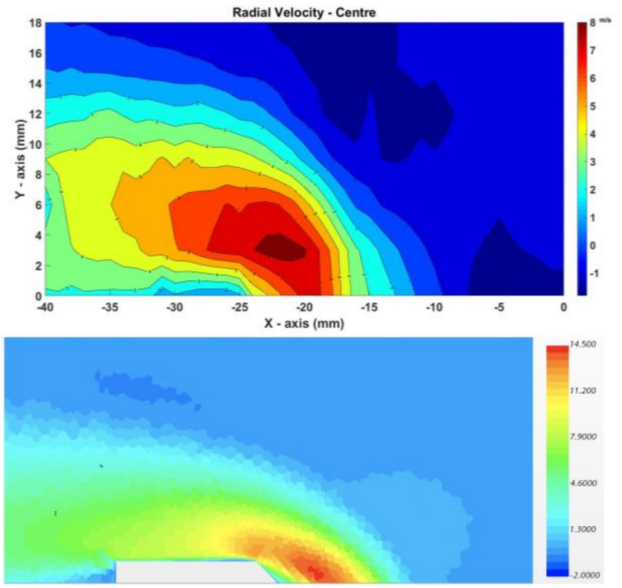

Figure 7 – Experimental (top) and numerical (bottom) profile of the radial (i) velocity magnitude vector on the axial plane

Of all planes, the most discrepancy in experimental and numerical predictions could be seen in the tangential velocity vector (Figure 8). It is believed that this is due to the positioning of the cross-section of the burner 1/3 section and the comparatively lower position of the jet in the numerical simulation.

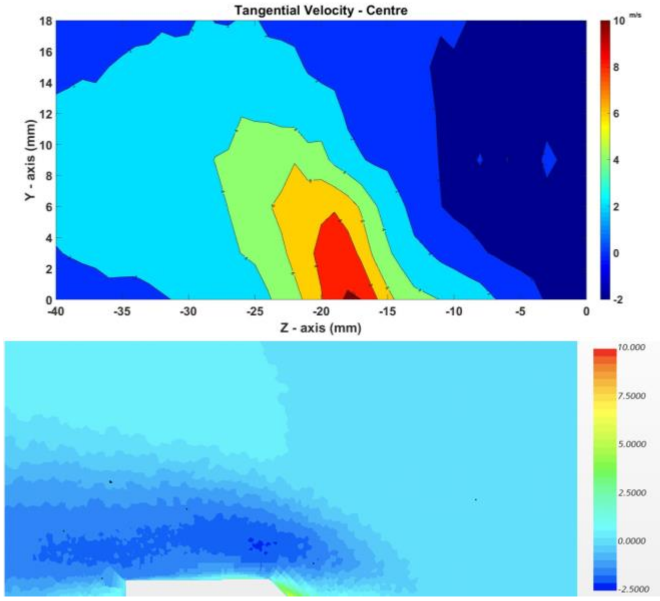

Figure 8 – Experimental (top) and numerical (bottom) profile of the tangential (j) velocity vector on the axial plane

Therefore, while velocity trends were in good agreement for the axial vector, further improvements could be made to adjust the position of the jet higher to correspond with experimental results. This discrepancy could be due to boundary layer effects at the burner walls and can be targeted by improving near wall mesh resolution or with an alternative model that is able to solve the near wall behavior more accurately.

Conclusions

This study reports the hydrodynamic performance of a novel design NIK15 burner, optimized for combustion of rich ammonia-hydrogen flames.

The results show a promising flow profile with a flat, anchored flame, a central recirculation zone and increased residence times. A RANS computational fluid dynamics simulation utilising the realizable k-epsilon model was shown to have good correlations with experimental results, though the jet position location was slightly lower than in the experimental results. The best correlations were seen in the axial velocity vector with most discrepancy in the tangential velocity vector.

This gives confidence to continue the progression with the existing mesh and physics models to more advanced simulations, such as the addition of chemistry solvers.

Acknowledgements

This work was supported by funding from the EPSRC SAFE project (EP/ T009314/1). The authors also thank Mr Malcolm Seaborne for his expertise in the development of the experimental facilities used in this study.

References

[1] A. Valera-Medina, H. Xiao, M. Owen-Jones, W.I.F. David, P.J. Bowen, Ammonia for power, Prog. Energy Combust. Sci. 69 (2018) 63–102.

[2] P. Arsenie, G. Martinas, C. Gheorghe, A. Arsenie, Technologies for the Reduction of Nitrogen Oxides Emissions, TransNav, Int. J. Mar. Navig. Saf. Sea Transp. 9 (2015) 251–256.

[3] H. Kobayashi, A. Hayakawa, K.D.K.A. Somarathne, E.C. Okafor, Science and technology of ammonia combustion, Proc. Combust. Inst. 37 (2019) 109–133.

[4] A. Valera-Medina, M. Gutesa, H. Xiao, D. Pugh, A. Giles, B. Goktepe, R. Marsh, P. Bowen, Premixed ammonia/hydrogen swirl combustion under rich fuel conditions for gas turbines operation, Int. J. Hydrogen Energy. 44 (2019) 8615–8626.

[5] D. Pugh, J. Runyon, P. Bowen, A. Giles, A. Valera-Medina, R. Marsh, B. Goktepe, S. Hewlett, An investigation of ammonia primary flame combustor concepts for emissions reduction with OH*, NH2* and NH* chemiluminescence at elevated conditions, Proc. Combust. Inst. (2020).

[6] M. Guteša Božo, A. Valera-Medina, Prediction of Novel Humified Gas Turbine Cycle Parameters for Ammonia/Hydrogen Fuels, Energies. 13 (2020).

[7] M. Guteša Božo, S. Mashruk, S. Zitouni, A. Valera-Medina, Humidified ammonia/hydrogen RQL combustion in a trigeneration gas turbine cycle, Energy Convers. Manag. 227 (2021) 113625.

[8] S. Mashruk, H. Xiao, A. Valera-Medina, Rich-Quench-Lean model comparison for the clean use of humidified ammonia/hydrogen combustion systems, Int. J. Hydrogen Energy. 46 (2021) 4472–4484.

[9] O. Kurata, N. Iki, T. Matsunuma, T. Inoue, T. Tsujimura, H. Furutani, H. Kobayashi, A. Hayakawa, Performances and emission characteristics of NH3–air and NH3CH4–air combustion gas-turbine power generations, Proc. Combust. Inst. 36 (2017) 3351–3359.

[10] O. Kurata, N. Iki, T. Inoue, T. Matsunuma, T. Tsujimura, H. Furutani, M. Kawano, K. Arai, E.C. Okafor, A. Hayakawa, H. Kobayashi, Development of a wide range-operable, rich-lean low-NOx combustor for NH_3 fuel gas-turbine power generation, Proc. Combust. Inst. 37 (2019) 4587–4595.

[11] K.D.K.A. Somarathne, S. Hatakeyama, A. Hayakawa, H. Kobayashi, Numerical study of a low emission gas turbine like combustor for turbulent ammonia/air premixed swirl flames with a secondary air injection at high pressure, Int. J. Hydrogen Energy. 42 (2017) 27388–27399.

[12] E.C. Okafor, K.D.K.A. Somarathne, A. Hayakawa, T. Kudo, O. Kurata, N. Iki, H. Kobayashi, Towards the development of an efficient low-NOx ammonia combustor for a micro gas turbine, Proc. Combust. Inst. 37 (2019) 4597–4606.

[13] R.C. Rocha, M. Costa, X.S. Bai, Combustion and Emission Characteristics of Ammonia under Conditions Relevant to Modern Gas Turbines, Combust. Sci. Technol. 00 (2020) 1–20.

[14] H. Nozari, G. Karaca, O. Tuncer, A. Karabeyoglu, Porous medium based burner for efficient and clean combustion of ammonia–hydrogen–air systems, Int. J. Hydrogen Energy. 42 (2017) 14775–14785.

[15] D. del Olmo Diaz, D.F. Hinz, Performance of eddy-viscosity turbulence models for predicting swirling pipe-flow: Simulations and laser-Doppler velocimetry, ArXiv E-Prints. (2015) arXiv:1507.04648.

[16] European Commission, Industrial Emissions Directive, (2010).